

Electronic states of laterally coupled quantum rings

J. Planelles¹, F. Rajadell¹, J.I. Climente^{2,1}, M. Royo¹ and J.L. Movilla¹

¹Departament de Ciències Experimentals, UJI, Box 224, E-12080 Castelló, Spain

²CNR-INFM S3, Via Campi 213/A, 41100 Modena, Italy

E-mail: josep.planelles@exp.uji.es

Abstract.

The conduction band electron states of laterally-coupled semiconductor quantum rings are studied within the frame of the effective mass envelope function theory. We consider the effect of axial and in-plane magnetic fields for several inter-ring distances, and find strong changes in the energy spectrum depending on the coupling regime. Our results indicate that the magnetic response accurately monitors the quantum ring molecule dissociation process. Moreover, the anisotropic response of the electron states to in-plane magnetic fields provides information on the orientation of the quantum ring molecule.

1. Introduction

Quantum rings (QRs) stand as an alternative to quantum dots (QDs) as zero-dimensional structures for eventual use in nanotechnology devices. The main differences between the physics of QRs and that of QDs follow from the doubly-connected geometry of the rings, which provides them with a characteristic electronic shell structure, magnetic field response and transport properties.[1, 2, 3] While much attention has been devoted in the last years to the study of 'artificial molecules' made of coupled QDs (see e.g. Refs.[4, 5, 6] and references therein), only recently their QR counterparts have started being addressed. A number of experimental and theoretical works have studied vertically-coupled[7, 8, 9], and concentrically-coupled[10, 11, 12, 13] QRs. Conversely, to our knowledge, laterally-coupled quantum rings (LCQRs) have not been investigated yet. This is nonetheless an interesting problem: on the one hand, LCQRs constitute 'artificial molecules' with unique topology (two LCQRs may be triply-connected), what should be reflected in unique energy structures; on the other hand, the formation of pairs of LCQRs in the synthesis of self-assembled QRs is apparent.[14] Therefore, one could investigate LCQRs experimentally by probing spectroscopically the response of selected individual entities from a macroscopic sample of self-assembled QRs, as done e.g. in Ref.[15] for single QRs.

In this work we study the conduction band single-electron energy levels and wave functions of a pair of nanoscopic LCQRs, as a function of the distance between the two constituent QRs. Particular emphasis is placed on the effect of external magnetic fields, applied along the axial and two transversal in-plane directions, which lead to characteristic magnetic responses depending on the strength of the inter-ring coupling regime.

2. Theoretical considerations

Since usual QRs have much stronger vertical than lateral confinement,[2] we calculate the low-lying states of LCQRs using a two-dimensional effective mass-envelope function approximation Hamiltonian which describes the in-plane ($x - y$) motion of the electron in the ring. In atomic units, the Hamiltonian may be written as:

$$H = \frac{1}{2m^*}(\mathbf{p} + \mathbf{A})^2 + V(x, y) \quad (1)$$

where m^* stands for the electron effective mass and $V(x, y)$ represents a finite scalar potential which confines the electron within the lateral limits of the double ring heterostructure. Here we define x as the direction of dissociation of the LCQRs. \mathbf{A} is the vector potential, whose value depends on the orientation of the magnetic field B . Actually, the choice of \mathbf{A} is limited by the requirement that it should make it possible to separate ($x - y$) coordinates from z in the Hamiltonian.[16] Within the Coulomb gauge, for a field applied along z (axial magnetic field), this is fulfilled e.g. by $\mathbf{A}_{\mathbf{B}_z} = (-y, x, 0)\frac{1}{2}B$. For an in-plane magnetic field applied along x (y), this is fulfilled e.g. by $\mathbf{A}_{\mathbf{B}_x} = (0, 0, y)B$ ($\mathbf{A}_{\mathbf{B}_y} = (0, 0, -x)B$). Replacing these values of the vector potential in Hamiltonian (1) we obtain:

$$H(B_z) = \frac{\hat{p}_{\parallel}^2}{2m^*} + \frac{B_z^2}{8m^*}(x^2 + y^2) - i\frac{B_z}{2m^*}\left(x\frac{\partial}{\partial y} - y\frac{\partial}{\partial x}\right) + V(x, y), \quad (2)$$

$$H(B_x) = \frac{\hat{p}_{\parallel}^2}{2m^*} + \frac{B_x^2}{2m^*}y^2 + V(x, y), \quad (3)$$

$$H(B_y) = \frac{\hat{p}_{\parallel}^2}{2m^*} + \frac{B_y^2}{2m^*}x^2 + V(x, y). \quad (4)$$

The eigenvalue equations of Hamiltonians (2-4) are solved numerically using a finite-difference method on a two-dimensional grid (x, y) extended far beyond the LCQR limits. This discretization yields an eigenvalue problem of a huge asymmetric complex sparse matrix that is solved in turn by employing the iterative Arnoldi factorization.[17]

In this work we investigate nanoscopic laterally-coupled GaAs QRs embedded in an $\text{Al}_{0.3}\text{Ga}_{0.7}\text{As}$ matrix. We then use an effective mass $m^*=0.067$ and a band-offset of 0.262 eV.[18] The pair of rings which constitute the artificial molecule have inner radius $r_{in} = 12$ nm and outer radius $r_{out} = 16$ nm, and the separation between their centers is given by the variable d .

3. Results and discussion

3.1. Zero magnetic field

We start by studying the electron wave function localization in LCQRs for increasing inter-ring distances, from the strongly coupled to the weakly coupled regime (a process we shall hereafter refer to as *dissociation of the quantum ring molecule*), in the absence of external fields. Figure 1 illustrates the wave functions of the three lowest-lying electron states for several values of d . The corresponding profiles of the confining potential barrier are also represented using dotted lines. When the QRs are strongly coupled ($d = 12$ nm), one clearly identifies a s -like ground state and two p -like excited

states. The states localize along the arms of the LCQRs, as if in a single elliptical QR, with some excess charge deposited in the region where the two QRs overlap. As the inter-ring distance increases, the available space in the overlapping regions first increases. This tends to localize the ground and first excited states in such regions ($d = 18$ nm) until they eventually become the even and odd solutions of a double quantum well ($d \sim 26$ nm). For further increased inter-ring distance, an inner arm of the LCQRs is formed. As a result, the ground state tends to localize along it ($d = 28$ nm), thus benefiting from a reduced centrifugal energy. Meanwhile, the first excited state, which is not so prone to minimize centrifugal forces due to its p -like symmetry, prefers to spread along the external arms of the rings. Finally, for longer inter-ring distances, the QRs start detaching. When the rings are close to each other, tunneling between the two structures is significant and the ground state remains localized mostly in the middle of the LCQRs ($d = 36$ nm), but it soon evolves into the ground state of single QRs, with a tunneling acting as a small perturbation ($d = 38$ nm). All along the dissociation process, the second and higher excited states remain relatively insensitive to changes in d due to their larger kinetic energy.

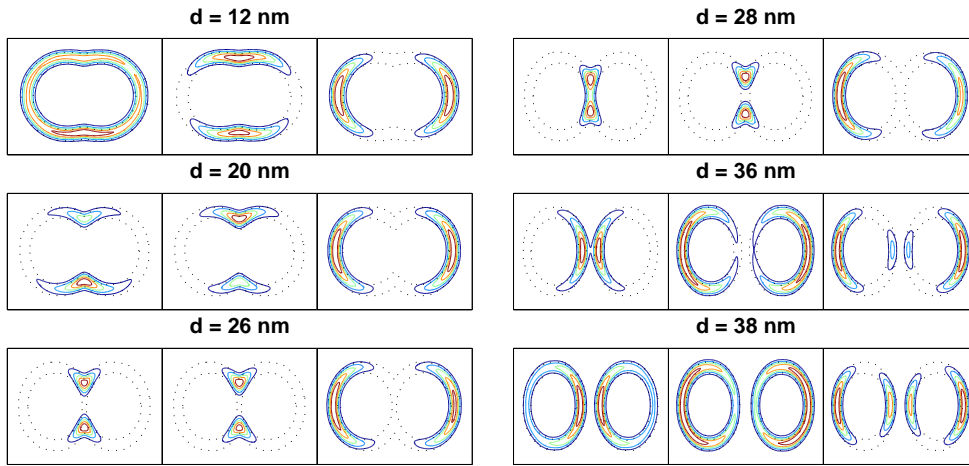


Figure 1. (Color online). Contours of the wave functions corresponding to the three lowest-lying electron states (from left to right) of LCQRs with different inter-ring distance d at $B = 0$. Dotted lines denote the confinement potential profile.

3.2. Effect of external magnetic fields

We next study the response of the electron energy levels to external magnetic fields. In general, the magnetic response can be understood from the $B = 0$ charge distribution described in the previous section. This is particularly clear in the case of an axial magnetic field, where the field barely squeezes the wave functions shown in Fig.1. To illustrate this, let us analyze Figure 2, which depicts the low-lying energy levels against B_z for several inter-ring distances. For $d = 12$ nm, the picture resembles the usual Aharonov-Bohm spectrum of single QRs,[1, 16] save for the anticrossings appearing between sets of two consecutive energy levels. These are due to the fact that the electron states no longer have circular (C_∞) symmetry as in single QRs, but

rather elliptical (C_2) one. Therefore, the pairs of eigenvalues which cross one another correspond to the two irreducible representations of the C_2 symmetry group. As d increases and the confining potential elongates, the anticrossing gaps become larger. Moreover, as the two lowest-lying states tend to become the even and odd solutions of a double quantum well, they become nearly degenerate and, being less efficient to trap magnetic flux, the amplitude of their energy oscillations is reduced (see panel corresponding to $d = 20$ nm in Fig. 2). In the next stage, around $d = 28$ nm, the ground state localizes to a large extent along the middle arm of the LCQRs and it takes essentially a singly-connected shape, thus preserving a QD-like magnetic response. On the other side, the first excited state tends to retrieve the p -like symmetry. Therefore, its energy and magnetic behavior become similar to that of the second QD excited state. In the last stage, when the QRs are already detached and the ground state wave function starts delocalizing among the two structures ($d = 36 - 38$ nm), the magnetic response is essentially that of a single QR with a perturbation arising from the tunneling between the rings, which rapidly diminishes with d . Notice that in this weak-coupling limit, the period of the Aharonov-Bohm oscillations is larger than in the strongly coupled limit. This is due to the smaller area of the inner holes of the individual rings as compared to that of the strongly coupled structure.

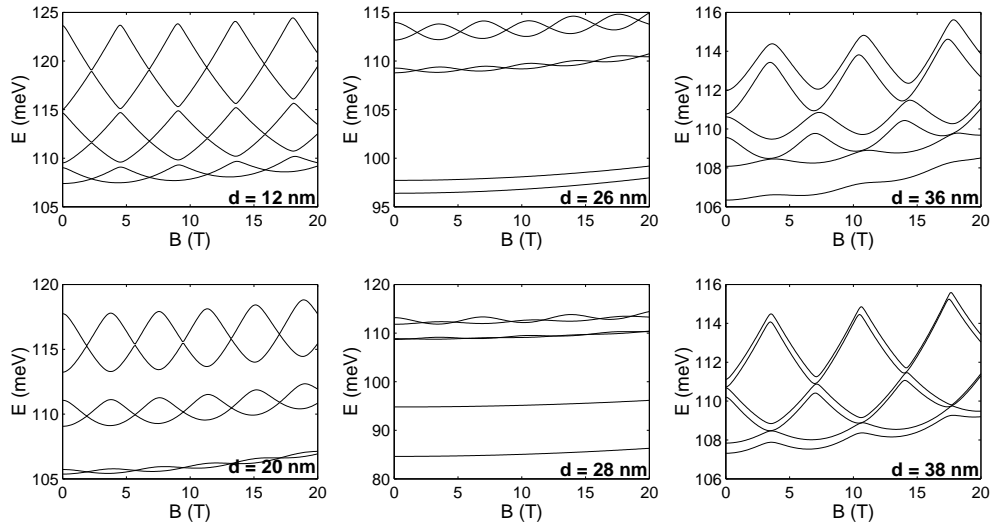


Figure 2. Low-lying electron energy levels vs axial magnetic field in LCQRs with different inter-ring distance.

Figures 3 and 4 show the energy levels against in-plane magnetic fields directed along the x and y directions, respectively. B_x is applied along the dissociation axis and it tends to squeeze the electron wave function in the y direction. The opposite holds for B_y . In both cases, when the QRs are strongly coupled ($d = 12 - 20$ nm) the effect of the field is to form pairs of degenerate energy levels. These are the even and odd solutions of double quantum wells building up in the longitudinal (B_x) or transversal (B_y) edges of the ring structure, as illustrated in the insets of the figures for the lowest-lying states. The formation of double well solutions at moderate values of in-plane magnetic fields has been also reported for nanoscopic single QRs.[16] An additional feature is however present in LCQRs, because the asymmetric confinement

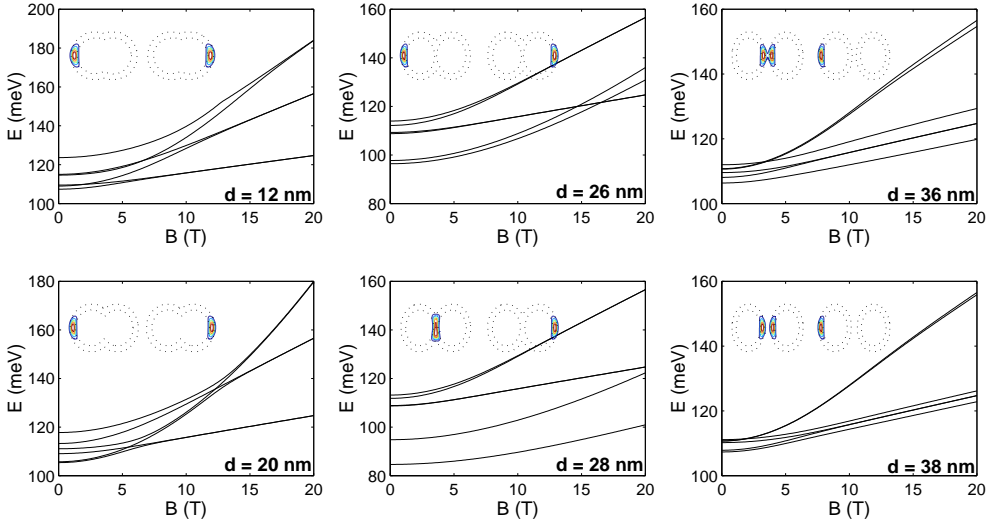


Figure 3. (Color online). Low-lying electron energy levels vs in-plane magnetic field in LCQRs with different inter-ring distance. The field is applied parallel to the dissociation axis. The insets show the wave functions of the two lowest-lying electron states (from left to right) at $B = 20$ T.

in the x and y directions leads to anisotropic magnetic response. As a result, for instance, one observes that the values of the field at which the double quantum well solutions are obtained are much smaller for B_y than for B_x . Thus, the two lowest-lying states at $d = 12$ nm become degenerate at $B \sim 5$ T for B_y , while they do so at $B \sim 8$ T for B_x . Another difference in the spectrum is the presence of crossings between given energy levels for B_x (e.g. between the first and second excited states), which are missing for B_y . This is because the two p -like states of the strongly coupled QRs are non-degenerate at zero magnetic field, due to the eccentricity of the LCQR system, and the applied field may reverse their energy order depending on the direction. When the coupling between the LCQRs is intermediate ($d \sim 26$ nm), the states which at $B = 0$ have singly-connected wave functions behave as in QD, i.e. they depend weakly on the external field. On the contrary, the doubly-connected states keep on behaving as in a QR, i.e. they tend to form double quantum well solutions. Finally, for weakly coupled QRs ($d \sim 38$ nm), different limits are reached depending on the in-plane magnetic field direction. B_y strongly enhances tunneling between the two QRs, so that the lowest-lying states are double well solutions mostly localized in the vicinity of the tunneling region (see insets in Fig. 4). Conversely, for B_x double well solutions localized either in the inner or in the outer edges of the QRs alternate (see insets in Fig. 3).

4. Conclusions

We have studied the electron states of nanoscopic LCQRs as a function of the inter-ring distance and external magnetic fields. The wave function localization at $B = 0$ changes dramatically depending on the inter-ring distance, and this gives rise to characteristic magnetic responses for strong, intermediate and weak coupling regimes.

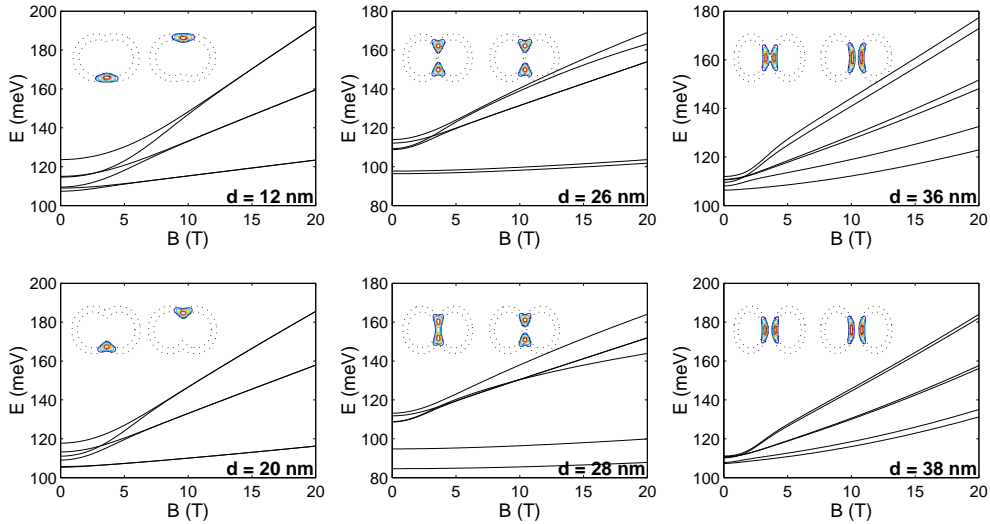


Figure 4. (Color online). Low-lying electron energy levels vs in-plane magnetic field in LCQRs with different inter-ring distance. The field is applied perpendicular to the dissociation axis. The insets show the wave functions of the two lowest-lying electron states (from left to right) at $B = 20$ T.

Moreover, a clearly anisotropic response is found for in-plane fields applied parallel or perpendicular to the LCQRs dissociation direction. These results suggest that probing spectroscopically the magnetic response of electrons in LCQRs may provide valuable information on the strength of coupling and the orientation of the QR molecule.

Acknowledgments

Financial support from MEC-DGI project CTQ2004-02315/BQU and UJI-Bancaixa project P1-B2002-01 is gratefully acknowledged. J.I.C. has been supported by the EU under the Marie Curie IEF project MEIF-CT-2006-023797 and the TMR network “Exciting”.

- [1] Viefers S, Koskinen P, Deo PS, and Manninen M, *Physica E* **21**, 1 (2004), and references therein.
- [2] Lee BC, Voskoboynikov OP, and Lee CP, *Physica E* **24**, 87 (2004), and references therein.
- [3] Neder I, Heiblum M, Levinson Y, Mahalu D, and Umansky V, *Phys. Rev. Lett.* **96**, 016804 (2006).
- [4] Austing DG, Sasaki S, Muraki K, Tokura Y, Ono K, Tarucha S, Barranco M, Emperador A, Pi M, and Garcias F, Chapter 2 in *Nano-Physics & Bio-Electronics: A New Odyssey*, Elsevier (2002).
- [5] DiVicenzo DP, *Science* **309**, 2173 (2005).
- [6] Jaskolski W, Bryant GW, Planelles J, and Zielinski M, *Int. J. Quantum Chem.* **90**, 1075 (2002).
- [7] Granados D, Garcia JM, Ben T, and Molina SI, *Appl. Phys. Lett.* **86**, 071918 (2005); Suarez F, Granados D, Dotor ML, and Garcia JM, *Nanotechnology* **15**, S126 (2004).
- [8] Climente JJ, and Planelles J, *Phys. Rev. B* **72**, 155322 (2005).

- [9] Malet F, Barranco M, Lipparini E, Mayol R, Pi M, Climente JI, and Planelles J, to be published in *Phys. Rev. B* (2006).
- [10] Mano T, Kuroda T, Sanguinetti S, Ochiai T, Tateno T, Kim J, Noda T, Kawabe M, Sakoda K, Kido G, and Koguchi N, *Nanoletters* **5**, 425 (2005); Kuroda T, Mano T, Ochiai T, Sanguinetti S, Sakoda K, Kido G, and Koguchi N, *Phys. Rev. B* **72**, 205301 (2005).
- [11] Szafran B, and Peeters FM, *Phys. Rev. B* **72** 155316 (2005).
- [12] Planelles J, and Climente JI, *Eur. Phys. J. B* **48**, 65 (2005).
- [13] Climente JI, Planelles J, Barranco M, Malet F, Pi M, to be published in *Phys. Rev. B* (2006).
- [14] Lee BC, and Lee CP, *Nanotechnology* **15**, 848 (2004); Schramm A, Kipp T, Wilde F, Schaefer J, Hyen Ch, and Hansen W, *J. Cryst. Growth* **289**, 81 (2006).
- [15] Warburton RJ, Schaflein C, Haft D, Bickel F, Lorke A, Karrai K, Garcia JM, Schoenfeld W, and Petroff PM, *Nature* **405**, 926 (2000).
- [16] Planelles J, Climente JI, and Rajadell F, to be published in *Physica E* (2006).
- [17] Arnoldi WE, *Quart. J. Applied Mathematics* **9**, 17 (1951); Saad Y, *Numerical Methods for large Scale Eigenvalue Problems* (Halsted Press, New York, 1992); Morgan RB, *Math. Comp.* **65**, 213 (1996).
- [18] Yamagiwa M, Sumita N, Minami F, and Koguchi N, *J. Lumin.* **108**, 379 (2004).